*Research Article*

# A grading method for analyzing internal erosion processes of nano-silica improved sand

## Mayao Cheng[1], Yang Zeng[2,*], Linsheng Chen[1], Hong Yang[1]

[1]School of Transportation and Civil Engineering &Architecture, Foshan University
Guangyun Road 33, Foshan City 528225, China
[2]School of Highway, Chang'an University
Middle Section of Nan'er Huan Road, Xi'an 710064, China
*e-mail:zy18882017394@163.com

Abstract: Internal erosion (IE) often occurs in poorly graded sand, one of the traditional treatments is reducing the permeability by grouting. In recent years, nano-silica becomes a choice of grouting materials as its low viscosity and good penetration capacity. According to present literature, the effect of decreasing loss mass during IE of fine sand and nano-silica improved sand (NIS) was rarely studied. One of the important reasons is that, mass loss during IE was previously focused on and was weighed after filtering the effluent by electronic balance. More accurate weighing method should be studied, because electronic balance can not accurately weigh fine particles. In this paper, nano-silica not only acted as the grouting material but also acted as the IE process signal. So, a new grading method was conducted to monitor the particle size distribution in the effluent and illustrate the process of IE. Erosion time and permeability were also recorded and analyzed as comparison. The experimental results showed that the grading method can monitor precisely the diameter of loss particles and the composition of the effluent, grading range of 1-1000 μm can be adopted to monitor the coagulation of silica gel particles (1-50 μm, average diameter 11±5 μm) and fine sand particles (50-100 μm, average diameter 65±7 μm), grading range of 1-1000 nm can be adopted to monitor the smaller coagulation of silica gel particles (concentrated in the range of 1-250 nm). Through grading method, the IE of NIS can be divided into three stages: Removal and release of unbonded nano-silica particles and unbonded fine particles; Movement and discharge of bonded particles; Expansion of pores and instability of the whole sample skeleton.

Keywords: Internal erosion; Nano-silica imrpoved sand; Particle size analysis; Grading method

## I. INTRODUCTION

IE is one of the most common failures which threatens dams, tunnels and levees [1-5]. Soil nature and states determine the vulnerability of materials and govern the rate of IE. Under the IE influence, poorly graded soil will destabilize step by step with internal fine particles discharging through the network [6-7]. Three steps of IE were identified by Muresan et al [8].

- Firstly, internal defects gradually develop under hydraulic power (such as particle removal results in cumulative faults or displacements).
- Secondly, progress of suffusion, fine particles are ensnared to the pore of larger particles.

- Thirdly, extended pores or channels that are eroded backward.

Masi et al [9] monitored IE processes by time-lapse electrical resistivity tomography, and found that IE was a highly nonlinear dynamic process with time. Actually, some unimpressive evidences (like minor fissures, slides and depressions) were observed in the process of IE, while in rare cases, apparent geomorphic evidence could be found. For example, there are no abnormalities in dams at the beginning of IE, but the dams may collapse within a few hours with the lower toe of the levee begins to discharge like a spring. As the highly nonlinear dynamic process and hidden property of IE, it is important to monitor and analyze the process of IE using effective methods, and it is necessary to prevent the development of IE using appropriate control method.

Grouting were widely used to reduce the permeability of soil (grouting materials such as: cement, microfine cement, sodium silicate, organic polymers et al.). Indraratna et al [10] used lignosulfonate and cement as stabilizers, mixed with silt and compacted. Their results showed that the ability of erosion resistance of the improved silt was effectively improved. In order to improve the erosion resistance of slope soil, Pei et al [11] injected different concentrations of modified sodium carboxymethyl cellulose into the soil, their results showed that the water stability, shear strength and permeability coefficient of slope soil were effectively improved with the increase of concentration of modified sodium carboxymethyl cellulose. The best way to strengthen the soil of urban areas or historic sites was low-pressure grouting, the good penetration of sodium-silicate based material made it appropriate to low-pressure grouting, the viscosity and gelation time of sodium-silicate based material were controlled by adjusting the amount of catalyst [12]. These traditional materials are able to reduce permeability effectively and improve the strength of soil. But sometimes, the effect of controlling IE is not so ideal in certain conditions. For example, the particle diameters of cement-based slurries are mostly in the micron range, while the pores of fine/salty sands are in micron/nano scale, cement-based slurries can not effectively permeate through fine/salty sands. The outstanding rheological properties of sodium silicates and organic polymers, together with their low initials viscosities, facilitate permeation of soils as fine as silty sands. But sodium silicates have non-negligible shrinkage and insufficient durability, organic polymers are often toxic which will contaminate soil and groundwater.

Since the late 1980s, a new kind of materials called "nano-silica" has attracted attention in geotechnical Engineering, it has nano-scale particles, low viscosity, good penetration capacity, non-toxic and stable physicochemical properties [13-14]. Nano-silica was usually added in concrete to change the microstructure and bonding properties of cement slurry due to its high fineness and amorphous structure [15]. Nano-silica was also injected to improve the overall strength and stability of surrounding rock when the broken underground rock was excavated [16]. For prevent pollutant migration and saturated soil liquefaction, nano-silica could be grouted into ground to form anti-seepage barrier [17]. When nano-silica was used to improve loose sand, the literature shows that nano-silica could effectively reduce the pore volume of sand [18]. Nano-silica was mainly used as additive in concrete or injected with a small amount into soil/rock in the above applications. Nano-silica should be a good choice to prevent the internal erosion because of its nano-scale, especially for fine sand with micro pores inside. But as a new kind of grouting materials, nano-silica has not been used to prevent IE of fine sand yet, thus the anti-erodibility effect of nano-silica in fine sand has not been studied in the literature.

At present, research of IE process mainly focus on pure granular materials like silt, sand and gravel [19-22]. The understanding of IE phenomena relies mainly on laboratory experiments. Early experimental studies focused on the effect of particle size distribution in IE [23-24]. Then the spatial and temporal migration of fine particles were later recognized and qualitatively observed, and the axial displacement of tested soils under increased hydraulic gradient was measured quantitatively [25]. More recently, Fannin and Slanen [26], used mass loss, porosity change and permeability to distinct IE process. In previous IE tests, mass loss during IE was usually focused and was weighed by electronic balance, the effluent was collected, filtered and then dried to obtain the lost mass. If there were very fine particles in the effluent, it was hard to be collected and weighed. It is important to find an effective method to identify the process of IE when small particles in effluent is too hard to collect, filter and dry.

In view of the complexity of IE, the limitations of existing IE process monitoring techniques, and the micro/nano meter of NIS in IE, in this paper, a new grading method was conducted to study the IE process of NIS, and traditional drying method (weighing by electronic balance) was used for comparative analysis. In order to monitor the IE process of NIS, a series of the IE tests were performed on NIS. Two results can be obtained from the IE tests: Firstly, it might be possible to illustrate the development stages of IE of NIS by the grading method. Secondly, IE process of NIS was discrepancy with different curing time.

The structure of the paper is as follows. Section II introduces the related materials and method to realize the IE monitoring process of NIS. Section III gives results to measure the process of IE of NIS by the grading method. Finally, in Section IV, the conclusion is summarized.

## II. MATERIALS AND METHODS

### 1. Characteristics and compact process of sand sample

In embankment dams and levees, the liner and core material are usually composed by poorly graded sand [27]. Internal erosion is very likely to happen when the fines content is between 15% and 30% [28-29]. In our IE test, standard graded sand was adopted by mixing particles of different sizes, the grain size ranged from 50 to 400 µm, the particle size distribution is as same as that of Fell. The standard sand was washed before use and dried in an oven (the temperature should be between 105 °C and 110 °C).

The particle size distribution is shown in **Fig. 1**. The mixed sand was statically compacted in three layers, the final sand sample height was 100 mm. The physical properties of the sand samples are shown in **Table 1**. Internal erosion test was firstly conducted with sand sample before adding nano-silica, then water head and inflow velocity to achieve internal erosion were obtained.
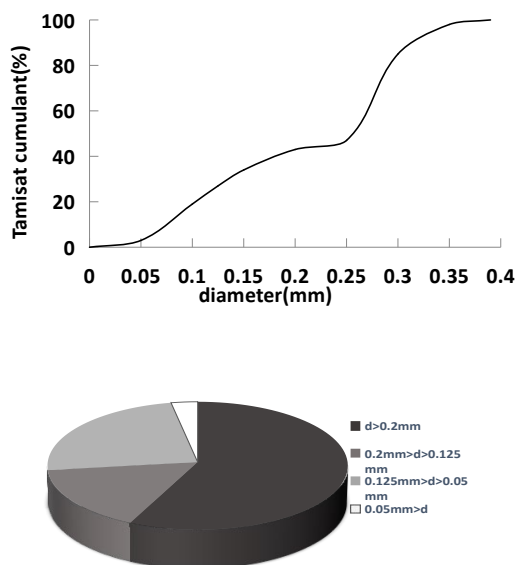


*Figure 1. Grain size curve and proportion of particles of different sizes*

*Table 1. Mineral composition and physical properties of sand samples*

| Sand properties | The mixed sands |
| --- | --- |
| Density (g/cm³) | 1.60 |
| Porosity | 0.38 |

## 2. Modified nano-silica sol

*Table 2. Basic physical properties of nano-silica sol and catalyst*

| Properties | Nano-silica | catalyst |
| --- | --- | --- |
| Dynamic viscosity (mPa.s) | 10 | 1 |
| Density (kg/L) | 1.1 | 1.07 |
| pH | 10 | 7 |
| Concentration (% by weight) | $SiO_2$ 15% | NaCl 10% |

## 3. The sample preparation process

In our experiment, the amount volumetric of colloidal silica was set to 25% of the pore volume of sand column. Therefore, the sand and the nano-silica were mixed together instead of grouting. The mixture was statically compacted in three layers, the

final sand column had a height of 100 mm and diameter of 50 mm. The porosity of sand columns after adding nano-silica was 0.29. The prepared columns were stored in the environment of 20 °C and 50% relative humidity for 2, 7 and 30 days. The NIS was designated as D2, D7 and D30 respectively. The initial permeabilities of D2, D7 and D30 were measured before IE test, which equalled $2.07\times10^{-6}$ m/s; $2.17\times10^{-6}$ m/s and $2.73\times10^{-6}$ m/s, respectively.

## 4. Testing apparatus

The IE test equipment consisted of water supply reservoir, inflow pump, hydraulic transducer, effluent reservoir and particle sizing analyser (**Fig. 2**). The IE tests were conducted at constant inflow rate (50 mL/min) from the top. Hydraulic transducers were conducted at the top and bottom of column to monitor the change of water head. NIS's weight and mass loss, distribution of particles and water head were recorded with the erosion time. The measuring range of hydraulic transducer was from 50 KPa to 2000 KPa, and the measurement accuracy was 0.10%. The size particles in effluent (from 0.01 to 100 μm) were measured by particle sizing analyzer. To reduce experiment error, all NISs were saturated before the scour experiment and each test result was obtained by 3 repeated tests.
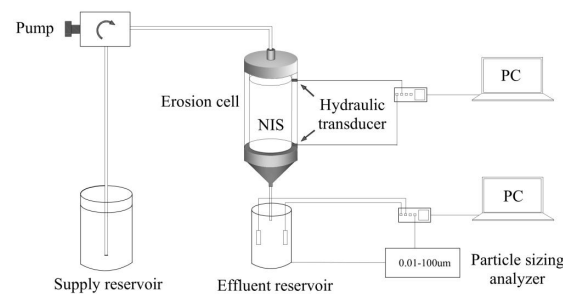


*Figure 2. Experimental set-up for internal erosion tests.*

## 5. Testing methods

To study the progress of IE, both the traditional drying method and the grading method were used at the same time. Test parameters include mass loss of NIS, porosity change and permeability change of NIS, size distribution of particles in the effluent.

### A. Loss of NIS quality

The mass loss of NIS was obtained by the traditional drying method. The loss particles were filtered at different time points by sieves which can get particles larger than 100 μm. The loss particles were dried at 90 °C for 24 hours and weighed at a 0.1 g scale. The real-time weight of NIS was obtained by subtracting the total mass of lost particles from the original weight of the sample.

### B. The porosity and permeability

The porosity is made up of two parts.

- when the particles remain stable without significant release, porosity is equal to the amount of inflow water.
- there exist newly formed pores and developing cracks. The quality of water in the void was determined by monitoring the NIS weights at a 0.1 g scale.

The increased volume of water in the pores can be obtained by dividing the mass of water by the density, So real-time porosity can be obtained. The permeability was obtained with Darcy law by measuring the velocity of inflow water and outflow water.

### C. Size distribution of loss particles

To obtain the size distribution of particles in the effluent, particles larger than 100 μm were collected by sieves that placed above the lower sump. These particles (diameter larger than 100 μm) were mainly composed of highly insoluble (silica coated) sand particles. The size distribution of particles (diameter smaller than 100 μm) was obtained by the grading method. The grading method was conducted by two particle sizing systems (PSS). For diameter ranging from 1 to 100 μm, the diameter and the number of particles were measured by single-particle optical sensing equipment (AccuSizer™ 780 optical PSS). These particles were constituted by sand particles and coagulation of silica gel particles. For diameter ranging from 1 to 1000 nm, the diameter and the number of particles were measured by dynamic light scattering equipment (Nicomp™ 380 PSS) . This range of particles was silica gel particles.

## III. RESULTS AND DISCUSSIONS

In advance of IE test of NIS, the IE test of unimproved sand was also conducted as comparison. Different inflow water rates were tested in the IE test of unimproved sand and NIS. For the unimproved sand: the IE developed very quickly under inflow rates of 10~40 mL/min; the granular structure of the unimproved sand sample was promptly destabilized under a inflow rate of 50 mL/min, the observed mechanism was not IE but quicksand, the cohesion between sand grains disappeared and notable amounts of sand were discharged within 1 minute. For the NIS, there was practically no IE phenomenon observed when the eroding fluid passing through at inflow rates of 10~40 mL/min. In order to obtain IE phenomenon of NIS, an constant inflow water rate of 50 mL/min was adopted.

### 1. The mass, the porosity and the permeability of NIS during IE

The mass of NIS and the mass of eroded particles (D2, D7 and D30) are exhibited in **Fig. 3(a)** and **Fig. 3(b)**. The results show three stages of IE.

- First stage of mass growth.

- second stage of plateau.
- last stage of mass loss.

Considering that the amount of particles flushed out in the early stage of the flushing experiment was large and changes rapidly, the measurement frequency at this stage was 5 min. In the subsequent long period of time, the internal structure of NIS was still relatively stable under the scouring of water flow, the lost particles were small in size and small in number, and the overall quality of NIS changes little. Therefore, this period of time was defined as the second stage in this paper, and the measurement frequency was 30 min.
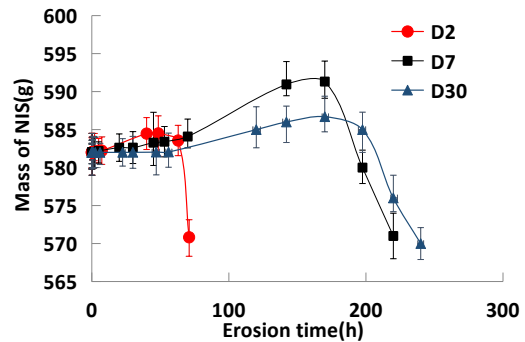


*(a) the mass variation*
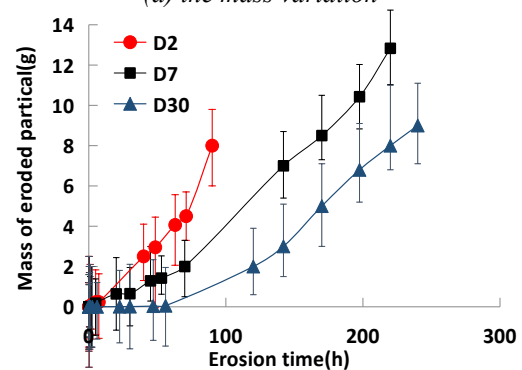


*(b) mass of eroded particles*

*Figure 3. Evolutions of: (a) the mass variation, and (b) mass of eroded particles of D2, D7 and D30, respectively.*

At the first stage, the mass of column grown with time {at t = $(0\sim144)\times10^3$ s for D2, $(0\sim511)\times10^3$ s for D7 and $(0\sim510)\times10^3$ s for D30}. The mass intake rates for D2, D7 and D30 were $1.71\times10^{-5}$ g.s$^{-1}$, $1.82\times10^{-5}$ g.s$^{-1}$ and $0.63\times10^{-5}$ g.s$^{-1}$ respectively. It can be deduced that in this stage, the unbonded nano-silica particles and unbonded fine particles began to move, more water flowed to the new holes and cracks.

At the second stage, the mass of column did not change with time {at t=$(144\sim230)\times10^3$ s for D2, $(511\sim612)\times10^3$ s for D7 and $(510\sim711)\times10^3$ s for D30}. It supported existence of the second IE stage of unimproved sand when the mass was balanced: On the one hand, the continuing discharge of fine particles; On the other hand, increasing mass of inflow water occupied the holes and cracks in the

column. The continuing time of the second stage was $201 \times 10^3$ s for D30, which was much longer than that for D2 and D7 ($86 \times 10^3$ s and $101 \times 10^3$ s, respectively). This phenomenon illustrated that, for D2, the improvement effect was not as good as D7 and D30. So, for the improved sand, the mass plateau of NIS meant no more mass loss, if this stage continued with time, no more IE happened, thus the nano-silica improvement was proved effective.

At the last stage, the curve of masses decayed quickly. The loss speed of mass was $97.05 \times 10^{-5}$ g.s$^{-1}$, $80.65 \times 10^{-5}$ g.s-1 and $66.26 \times 10^{-7}$ g.s-1 for D2, D7 and D30 respectively. It was clear that the IE developed the most quickly for D2, and the IE developed the most slowly for D30. That was to say, nano-silica was more effective for 7 or 30 days' curing.

The porosity and the permeability of NIS in different scouring times are exhibited in Fig. 4(a) and Fig. 4(b).
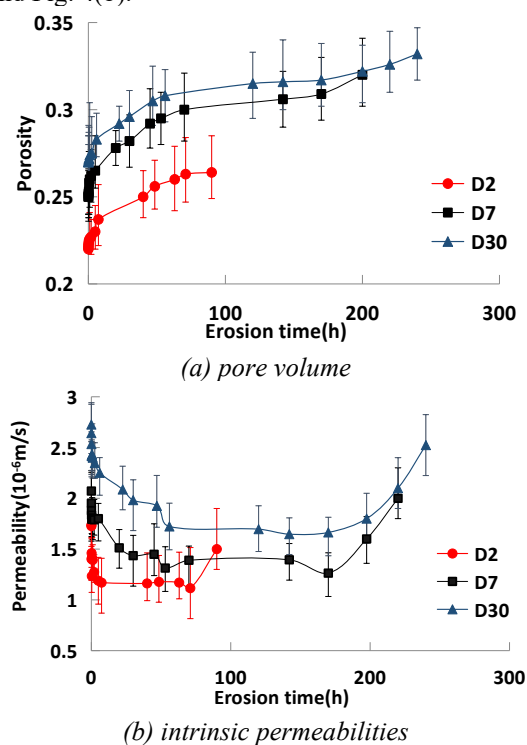


*(a) pore volume*



*(b) intrinsic permeabilities*

*Figure 4. Evolutions of: (a) pore volume, and (b) intrinsic permeabilities of D2, D7 and D30, respectively.*

In Fig. 4(a), the porosity during IE of D2, D7 and D30 are shown, we can summarize the following laws:

- At the first step, the porosity increased markedly, then the growth slowed down apparently, this law was consistent with the mass intake step which was obtained by mass analysis.
- At the second step, the curve tended to be flat, which showed that the sample structure was stable. The stabilization times lasted

$52 \times 10^3$ s, $360 \times 10^3$ s and $410 \times 10^3$ s for D2, D7 and D30, respectively. The differences of stabilization time were more sensitive by analyzing porosity than mass change of columns.

- At the last step, the rate of growth suddenly accelerated, which indicated the increase of porosity due to particle's flushing. The period was corresponding to mass loss analysis {at $(174.6-324) \times 10^3$ s for D2, $(594–720) \times 10^3$ s for D7 and $(612-864) \times 10^3$ s for D30}.

The failure stages of D7 and D30 were slower than that of sample D2. That was to say, nano-silica was more effective for 7 or 30 days' curing.

The permeability of sand was affected by the contraction geometry and the interconnections state between the pores. The result showed that the evolution of NIS permeability tended to decrease firstly, remained unchanged for a while and increased lastly. At the beginning of IE test, fine particles gradually moved under the action of inflow water, thus a temporary blockage of the pore channels happens in the bottom of NIS, which showed a rapid decrease of permeability. The similar law has been obtained in the references [30-32].

Then, after a period of stabilization, the permeability increased with the development of IE. The change law of permeability was mostly similar with that of mass and porosity, as all the factors were result from the three steps of IE development. But the permeability change was more sensitive in the first step due to the influence of blockage of fine particles in the bottom of sample. With the increased of curing time, the stabilizing time of second IE step increased. Compared with D2, the stabilizing time of D7 and D30 was longer, which indicated that the internal void's filling degree of D7 and D30 was higher.

## 2. The grading analysis of the effluent(1~1000 µm)

**Fig. 5(a-c)** shows the size composition (range of 1~1000 µm) of discharged particles during IE test. These particles were constituted by the coagulation of silical particles (1-50 µm, average diameter 11±5 µm) and fine sand particles (50-100 µm, average diameter 65±7 µm). The particle number of each size was precisely counted by AccuSizer™ 780 optical PSS, as a result, the particle number of each size was huge and was hard to show. The method of relative proportion method was adopted instead of showing numbers of particles.

Three factors are shown in each figure: erosion time, size of particles and occurrence probability. The numbers 0-10 above the chart represent the occurrence probability of the particles discharged during IE. The higher the number, the greater the

probability. On the other hand, it represents massive release of the particles with a certain size. The formula for the probability of occurrence is shown in (1).

$$p = 10\frac{d_n}{d_1} \qquad (1)$$

$n$ is the particle diameter (range of 1~1000 μm); $d_n$ represents the total number of particles greater than or equal to the particle size; $d_1$ represents the total number of particles with a particle diameter greater than or equal to 1 μm, that is, the total number of particles
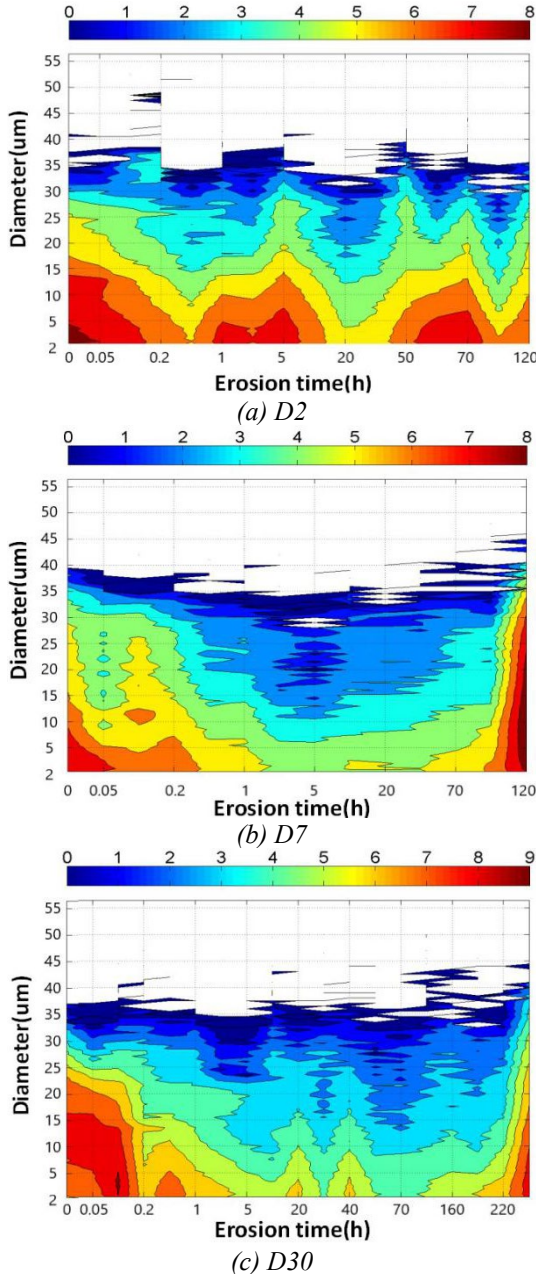


*(a) D2*



*(b) D7*



*(c) D30*

*Figure 5. Contributions of micrometric particles (finest sand sample grains + eroded silica gel particles) to the instantaneous discharged mass of NIS for IE tests with (a) D2, (b) D7, and (c) D30, respectively.*

Those tendencies were convex on both sides and concave in the middle. From quantitative perspective, those figures of D2, D7 and D30 showed that the discharges particle size was mostly concentrated in the range of 1-20, 1-15, 1-10 μm in first stage of IE (Lasting time about 1800 seconds). At the second stage, the corresponding discharged particles were concentrated in the range of 1-5 μm. At the last stage, the particles discharged rapidly, and the diameter of particle size was up to 80 μm. According to the results, those discharged particles demonstrated the continuous erosion. The weakening bonding effect of nano-silica leaded to the abundantly removal of fines and the subsequent instability of the coarse particles.

Those particles provided valuable information about IE dynamic evolution of NIS and the movement law of particles during IE. Particles discharged was mostly concentrated in the range of 1-20 μm in the first two steps of IE, which indicated that, the discharged particles were mostly the coagulation nano-silica which had less cohesive effect to sand particles and was easy to discharge. As indicated by previous results, most fine particles were initially fixed in closed pores or cavities, there were rare sand particles discharging in the first step of IE. Then, the swift released of particles bigger than 50 μm can be seen as signal of the discharge of fine sand particles the last stage. On the basis of those facts we can reach the following conclusion: After adding nano-silica, the development of IE was significantly delayed; The judgemental norm of IE step by proportion of fine sand particles should be raised; As well, more attention should be paid to the motoring the nano-silica discharged, and to study the cohesive effect of nano-silica; Nano-silica particles occupied a considerable part of 1-100 μm erosive particles either in the field of volume (70±8%, 79±8% and 73±15%, respectively) or mass (54±10%, 67±11% and 65±19%, respectively).

In Fig. 5(a-c), we can find that with the prolongation of curing time, the reinforcement effect of the samples gradually increased, and the erosion resistance time was prolonged. At the same flushing time point, the smaller the particle size and the smaller the number of flushed particles, which meant that the process of internal erosion was greatly slowed down and effectively suppressed with the prolongation of curing time.

## 3. The grading analysis of the effluent(1~1000 nm)

Fig. 6(a-c) shows the size composition (range of 1~1000 nm) of discharged particles during IE test. Monitoring the dynamic removal process of nano-silica particles was of great significance to study the seepage failure process of NIS. As nano-silica was nano-scale material, the nano-scale equipment (Nicomp™ 380 PSS) was used in trials to measure

the particle size distribution in the effluent. The results were shown in Fig. 6(a-c) with the same analytical method as the grading method for the effluent (particles range from 1 to 1000 nm).
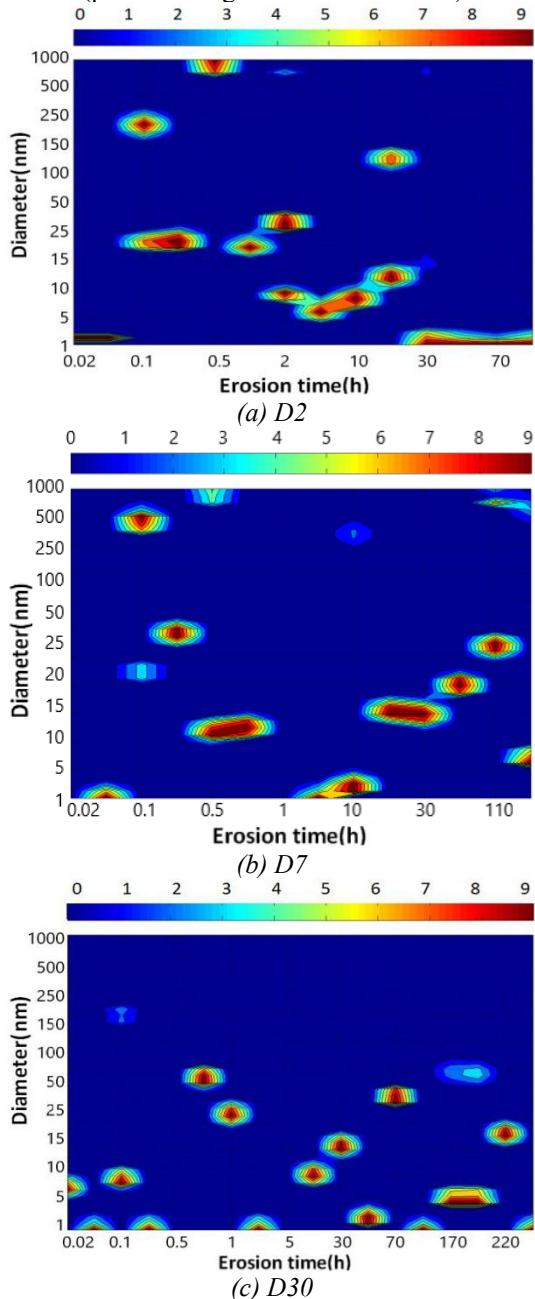

*(a) D2*


*(b) D7*


*(c) D30*

*Figure 6. Contributions of nanometric particles (eroded silica gel particles) to the instantaneous discharged mass of NIS for IE tests with (a) D2, (b) D7, and (c) D30, respectively.*

According to Kenney et al [33], when the size of the main channel of the filter structure is about 1/4 of the size of the particles that make up the filter structure in the pore network, fines can migrate in the channel. This means that the eroded silica gel particles (if the diameter is smaller than 11±5 μm) can pass through the narrow channel formed by the smallest particles of adjusted standard sand (average diameter of 65±7 μm). If the filling effect of nano-

silica sol is good, the internal pore size can be limited or the diameter of the pore diameter can be reduced, the aim of enhancing structural stability and restraining erosion can be achieved. So, the lower concentration of silica particles primarily reflects the high stability to resist erosion (such as: D30).

At the beginning of IE test, the unstable nano-silica particles separated from NIS. The particle discharged was generally larger (diameter of 1-200 nm for D2 and D7 due to short curing time, while the particle discharged was smaller (diameter of 1-50 nm for D30 with sufficient curing time. At the middle of IE test, the plateau step started and stopped at different times: $0.16{\sim}1.10{\times}10^5$ s for D2, $0.22{\sim}3.82{\times}10^5$ s for D7 and $0.11{\sim}7.02{\times}10^5$ s for D30. At this stage, the loss particle sizes of D2, D7 and D30 were concentrated in the range of 1-10 nm,1-15 nm and 1-20 nm, respectively. The rigid skeleton formed by particles and binder can effectively support the imposed seepage stresses. This indicated that silica fragments were hardly got rid of sample under the effect of cementation. At the last step of IE test, small nano-silica particles increased and some large particles appeared in the effluent, the time of large particles appearing were $(1.10-1.66){\times}10^5$ s for D2, $(3.82-4.14){\times}10^5$ s for D7 and $(7.02-8.46){\times}10^5$ s for D30, respectively), which matched reasonably with the beginning of fine sand particles discharged, the phenomenon implied that instability of NIS can be gauged by observing the occurrence of silica particles.

## 4. The dynamics of particle transport within NIS

Fig. 7(a-c) shows the largest micrometric particles (LMP; left scale) and the smallest nanometric particles (SNP; right scale) in the effluent. The LMP represents those particles that successfully separate from NIS. The movement is blocked when the particle diameter is larger than the internal network channel, while the size of the eroded particles is smaller than the internal channel of NIS, these particles will flow through the pore network with the injected water. Therefore, the change of LMP can be regarded as the evolution process of the internal network channel size. The SNP describes the finest silica that can be mechanically dislodged from the binder by seepage. A rule can be assumed that SNP sizes should be proportional with seepage stresses: i.e. coarser silica colloids would be dislodged at higher shear forces.

From the LMP data, the LMP value was about twice the value obtained by Kenney's formula (~55 μm) at the beginning of IE test. The reason was that those superficial, unfiltered sand grains are discharged firstly. Later, {at t=(0.61~7.20, 1.19~3.60 and 0.29~1.19)×10³ s for D2, D7 and D30, respectively}, The significant decreases of LMP signaled the further narrowing of the channel,

the minimal sizes of D2 rapidly tended to stabilize around 40~50 μm (70±1 and 60±3 μm for D7 and D30, respectively).
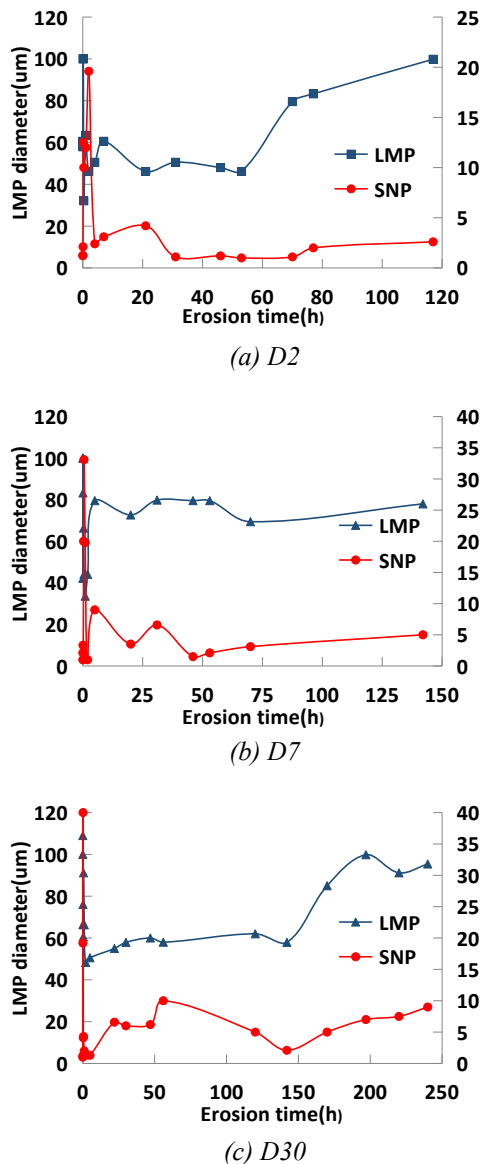


*(a) D2*



*(b) D7*



*(c) D30*

*Figure 7. Diameters of largest micrometric particles in effluent (LMP; left scales, filled circles) and smallest nanometric particles in effluent(SNP; right scales, empty circles) for IE tests with (a) D2, (b) D7, and (c) D30, respectively*

The diameter of the LMP was also maintained in a relatively stable range. SNP and LMP followed the similar laws. This phenomenon suggested that shear forces transfer some particles into the pore or network (such as unstable coarse silica fragments or sand grains) for partially blocking and filling the internal channels in early stage. Based on previous research and measured IE rates, the area of plateau not only described the low erodibility of NIS, but it also explained that the fine particles in motion (50~100 μm) were blocked by binder. At last, in the stage of mass loss, peaks of SNP matched with

higher concentrations of grains (50~100 μm) {at t = (2.77~4.21)×106 s for D2, (6.10~7.63) ×106 s for D7 and (6.12~9.11)×106 s for D30}. By comparing the quality change curve obtained by the traditional drying method, the data of the grading method and has been verified, and it is simpler and more exact.

With the prolongation of curing time, the reinforcement effect of NIS gradually increased, and the erosion resistance time was prolonged. At the same scouring time point, the smaller the particle size and the smaller the number of flushed particles, which meant that the process of internal erosion was greatly slowed down and effectively suppressed with the prolongation of curing time

## 5. Data synthesis

The grading method was conducted and compared with the traditional drying method. The IE development law of NIS was summarized.

- At the first stage, mass growth was related to the filling of pores by inflow water and the flushing of movable unbonded nano-silica particles and unbonded fine sand particles. At this step, through the grading method, it was found that the particle size of the lost particles decreased markedly.

- At the second stage, the internal structure of the sample was stable, the IE developed very slowly, while the size of particle in the effluent kept in a low value.

- At the last stage, the mass loss revealed the dynamic release of particles and the gradual instability of the rigid skeleton. The increase of porosity and permeability showed that pores or capillary channels developed significantly, and the range of particle size in the effluent increased significantly.

## IV. CONCLUSIONS

For soil with fine particles and small pores, grouting and monitoring the process of internal erosion is difficult. This research was planned and carried out with the purpose of filling the scientific gaps regarding the use of new method as replacement of the traditional drying method for monitoring IE of NIS. The laboratory research results of IE process of NIS were introduced. The grading method and the traditional drying method were compared and analyzed. The grading method can identify the process of IE of NIS by monitoring the distribution of particle size in the effluent with time. The process of IE of NIS can be divided into three stages:

- Removal and release of unbonded nano-silica particles and unbonded fine particles.
- Movement and discharge of bonded particles.

- Expansion of pores and instability of the whole sample skeleton.

Grading range of 1-1000 μm can be adopted to monitor the coagulation of silica gel particles (1-50 μm, average diameter 11±5 μm) and fine sand particles (50-100 μm, average diameter 65±7 μm). In the second stage, a large number of particles with 1-5 μm appeared, indicating that the internal structure of NIS began to be destroyed. In the third stage, when large particles with 50-100 μm appeared, NIS can no longer bear the damage of IE.

Grading range of 1-1000 nm can be adopted to monitor the smaller coagulation of silica gel particles (concentrated in the range of 1-250 nm). The range of particle size corresponding to the second stage is 1-20 nm. When the number of particles in this range rapidly decreased, it indicated that IE had entered the third stage and NIS was about to be destroyed..

With the extension of curing time, the impermeability of NIS improved, which can be judged by the appearance time of each particle size.

This study successfully demonstrate that the grading method is more accurate and simpler than traditional drying method for soil with fine particle and small pore size. So, for ensure the safety of the underground structure, it is necessary to monitor IE of NIS by the grading method in long time. We have to point out that only one graded sand sample is used in our research. the IE rule of NIS after 30 days of curing is also not considered. In the future research, we will gradually improve the grading method to test the improved soil with different grades and longer curing time.

## ACKNOWLEDGMENTS

## AUTHOR CONTRIBUTIONS

**M. Cheng**: Experiment, Investigation, Software, Data curation, Formal analysis, Writing-review & editing.

**Y. Zeng**: Experiment, Data analysis, Formal analysis, Writing-review & editing.

**L. Chen**: Experiment, Data analysis.

**H. Yang**: Investigation, Experiment.

## DISCLOSURE STATEMENT

The authors declare that they have no known competing financial interests or personal relationships that could have appeared to influence the work reported in this paper.

## REFERENCES

[1] M. Foster, R. Fell and M. Spannagle, The statistics of embankment dam failures and accidents. Canadian Geotechnical Journal 37 (5) (2000) pp. 1000-1024. https://doi.org/10.1139/t00-030

[2] M. Foster, R. Fell and M. Spannagle, Method for assessing the relative likelihood of failure of embankment dams by piping. Canadian Geotechnical Journal 37 (5) (2000) pp. 1025-1061. https://doi.org/10.1139/cgj-37-5-1025

[3] L. Caldeira, Internal Erosion in Dams: Studies and Rehabilitation. International Journal of Civil Engieering 17 (4) (2005) pp. 457-471. https://doi.org/10.1007/s40999-018-0329-5

[4] G. A. Fox and G. V. Wilson, The Role of Subsurface Flow in Hillslope and Stream Bank Erosion: A Review. Soil Science Society of America Journal 74 (6) (2010) pp. 717-733. https://doi.org/10.2136/sssaj2009.0319

[5] Correia et al, Experimental study on crack filling by upstream fills in dams. Géotechnique 64 (3) (2015) pp. 218-230. https://doi.org/10.1680/geot./14-P-198

[6] L. Ke and A. Takahashi, Strength reduction of cohesionless soil due to internal erosion induced by one-dimensional upward seepage flow. Soils & Foundations 52 (4) (2012) pp. 698-711. https://doi.org/10.1016/j.sandf.2012.07.010

[7] L. Ke and A. Takahashi, Triaxial Erosion Test for Evaluation of Mechanical Consequences of Internal Erosion. Geotechnical Testing Journal 37 (2) (2014). https://doi.org/10.1520/GTJ20130049

[8] B. Muresan, N. Saiyouri, A. Guefrech and P. Y. Hicher, Internal erosion of chemically reinforced granular materials: A granulometric approach. Journal of Hydrology 411 (3-4) (2011) pp.178-184. https://doi.org/10.1016/j.jhydrol.2011.09.009

[9] M. Masi, F. Ferdos, G. Losito, and L. Solari, Monitoring of internal erosion processes by time-lapse electrical resistivity tomography. Journal of Hydrology 589 (1) (2020) pp. 125340. https://doi.org/10.1016/j.jhydrol.2020.125340

[10] B. Indraratna, T. Muttuvel, H. Khabbaz and R. Armstrong, Predicting the erosion rate of chemically treated soil using a process simulation apparatus for internal crack erosion. Journal of Geotechnical and Geoenvironmental Engineering 134 (6) (2008) pp. 837-844. https://doi.org/10.1061/(ASCE)1090-0241(2008)134:6(837)

[11] X. J. Pei, Q. W. Yang, Q. Xu, X. C. Zhang, Y. Huang, Research on glue reinforcement mechanism and scouring resistant properties of soil slopes by modified carboxymethyl cellulose. Chinese Journal of Rock Mechanics and Engineering 35 (11) (2016) pp. 2316-2327. https://doi:10.13722/j.cnki.jrme.2015.1060

[12] G. Spagnoli, A review of soil improvement with non-conventional grouts. International Journal of Geotechnical Engineering 1 (15) (2018) pp. 273-287. https://doi.org/10.1080/19386362.2018.14846 03

[13] S. M. A. Zomorodian, S. Moghispoor, B. C. O'Kelly, S. S. Babaei, Improving internal erosion resistance of silty sand using additives. Dams and Reservoirs 30 (1) (2020) pp. 29-41. https://doi.org/10.1680/jdare.20.00007

[14] P. M. Gallagher and Y. Lin, Colloidal Silica Transport through Liquefiable Porous Media. Journal of Geotechnical and Geoenvironmental Engineering 135 (11) (2009) pp. 1702-1712. https://doi.org/10.1061/(ASCE)GT.1943-5606.0000123

[15] S. Francisco Santos, J. de Anchieta Rodrigues, G. H. Denzin Tonoli, A. E. F. de Souza Almeida, H. Savastano Jr, Effect of colloidal silica on the mechanical properties of fiber-cement reinforced with cellulosic fibers, Journal of Materials Science. 49 (2014) 7497-7506, https://doi.org/10.1007/s10853-014-8455-1

[16] K. G. Holter, H. O. Hognestad, Modern pre-injection in underground construction with rapid-setting microcements and colloidal silica – Applications in conventional and TBM-tunnelling, Geomechanics and Tunnelling. 5(1) (2012) 49-56, https://doi.org/10.1002/geot.201200001

[17] B. Iranpour, A. Haddad, The influence of nano-materials on collapsible soil treatment. Engineering Geology. 205 (2016) 40-53, https://doi.org/10.1016/j.enggeo.2016.02.015. T. C. Kenney and D. Lau, Internal stability of granular filters. Canadian Geotechnical Journal 22 (2) (1985) pp. 215-225. https://doi.org/10.1139/t85-029

[18] C. Todaro, Grouting of cohesionless soils by means of colloidal nanosilica. Case Studies in Construction Materials (15) (2021). https://doi.org/10.1016/j.cscm.2021.e00577

[19] L. M. Reddi, I. M. Lee, M. V. S. Bonala, Comparison of internal and surface erosion using flow pump tests on a sand-kaolinite mixture. Geotechnical Testing Journal 23 (1) (2000) pp.116-122. https://doi.org/10.1520/GTJ11129J

[20] F. Bendahmane, D. Marot and A. Alexis, Experimental Parametric Study of Suffusion and Backward Erosion. Journal of Geotechnical & Geoenvironmental Engineering 134 (1) (2008) pp. 57-67. https://doi.org/10.1061/(ASCE)1090-0241(2008)134:1(57)

[21] M. Ouyang and A. Takahashi, Influence of initial fines content on fabric of soils subjected to internal erosion. Canadian Geotechnical Journal 53 (2) (2016) pp. 299-313. https://doi.org/info:doi/10.1139/cgj-2014-0344

[22] M. Foster and R. Fell, Assessing Embankment Dam Filters That Do Not Satisfy Design Criteria. Journal of Geotechnical & Geoenvironmental Engineering 127 (5) (2001) pp. 398-407. https://doi.org/10.1061/(ASCE)1090-0241(2001)127:5(398)

[23] F. W. Chi and R. Fell, Assessing the Potential of Internal Instability and Suffusion in Embankment Dams and Their Foundations. Journal of Geotechnical & Geoenvironmental Engineering 134 (3) (2008) pp. 401-407. https://doi.org/10.1061/(ASCE)1090-0241(2008)134:3(401)

[24] R. Moffat, R. J. Fannin and S. J. Garner, Spatial and temporal progression of internal erosion in cohesionless soil. Canadian Geotechnical Journal 48 (3) (2011) pp. 399-412. https://doi.org/10.1139/T10-071

[25] R. J. Fannin and P. Slangen, On the distinct phenomena of suffusion and suffosion. Géotechnique Letters (4) (2014) pp. 289-294. https://doi.org/10.1680/geolett.14.00051

[26] D. Marot, F. Bendahmane, F. Rosquoet and A. Alexis, Internal flow effects on isotropic confined sand-clay mixtures. Soil Sediment Contam 18 (3) (2009) pp. 294-306. https://doi.org/10.1080/15320380902799524

[27] R. Fell, P. MacGregor, D. Stapledon and G. Bell, Geotechnical engineering of dams. (2005). https://doi.org/10.1201/NOE0415364409

[28] D. S. Chang and L. M. Zhang, Extended internal stability criteria for soils under seepage. Soils Found 53 (4) (2013) pp. 569-583. https://doi.org/10.1016/j.sandf.2013.06.008

[29] K. Boschi, C. G. Prisco and M. O. Ciantia, Micromechanical investigation of grouting in soil. International Journal of Solids and Structures (187) (2019) pp. 121-132. https://doi.org/10.1016/j.ijsolstr.2019.06.013

[30] Z. Hu, Y. D. Zhang and Z. X. Yang, Suffusion-induced deformation and microstructural change ofgranular soils: a coupled CFD-DEM study. Acta Geotechnica 14 (3) (2019) pp. 795-814.
https://doi.org/10.1007/s11440-019-00789-8

[31] Oueidat, Mohamad, A. Benamar and A. Bennabi, Effect of Fine Particles and Soil Heterogeneity on the Initiation of Suffusion.

Geotechnical and Geological Engineering 39 (3) (2021).
https://doi.org/10.1007/s10706-020-01632-8

[32] T. C. Kenney, R. Chahal, E. Chiu, G. I. Ofoegbu, G. N. Omange, and C. A. Ume. Controlling constriction sizes of granular filters. Canadian Geotechnical Journal 22 (1) (1985) pp. 98-98.
https://doi.org/10.1139/t85-005